CONFIDENTIAL

NACA RM L52L16

NACA

RESEARCH MEMORANDUM

A TRANSONIC WIND-TUNNEL INVESTIGATION OF THE EFFECTS OF LONGITUDINAL WING LOCATION AND VARYING BODY SIZE ON THE INTERFERENCE CHARACTERISTICS OF A 45° SWEPTBACK WING

By Donald L. Loving

Langley Aeronautical Laboratory
Langley Field, Va.

NATIONAL ADVISORY COMMITTEE
FOR AERONAUTICS

WASHINGTON

March 10, 1953

CONFIDENTIAL

NATIONAL ADVISORY COMMITTEE FOR AERONAUTICS

RESEARCH MEMORANDUM

A TRANSONIC WIND-TUNNEL INVESTIGATION OF THE EFFECTS OF LONGITUDINAL WING LOCATION AND VARYING BODY SIZE ON THE INTERFERENCE CHARACTERISTICS OF A 45° SWEPTBACK WING

By Donald L. Loving

SUMMARY

The effects of longitudinal location of the wing and varying body size on the interference characteristics of a 45° sweptback wing have been investigated over a Mach number range from 0.60 to 1.13 at angles of attack of 0°, 2°, 4°, and 7° in the Langley 8-foot transonic tunnel. The wing had an aspect ratio of 4, a taper ratio of 0.6, and NACA 65A006 airfoil sections. The wing was investigated at two longitudinal locations, 4 inches apart, on a body. Also, the wing was investigated on two differently sized bodies, one approximately 10 percent larger than the other.

The results obtained indicated that the zero-lift drag of the wing with interference in the forward position was lower throughout the Mach number range than for the wing with interference in the rearward position. The transonic drag rise of the wing with interference for lift coefficients up to 0.4 was reduced up to a Mach number of approximately 1.00 by moving the wing to the forward position. Lift and pitching-moment characteristics were not severely affected by a change in location of the wing for the test angle-of-attack range. The increase in body size decreased the zero-lift drag rise of the wing with interference from 30 to 50 percent in the transonic range and increased the average slope of the lift curve. The pitching-moment characteristics of the wing with interference were not severely affected by the change in body size.

INTRODUCTION

As part of a systematic wing-body interference investigation at transonic speeds, the first phases of which have been reported in

references 1 and 2, additional tests have been made to determine the effect on wing with interference characteristics of two longitudinal positions of a 45° sweptback wing on a body. Other tests have been made to investigate the effect on wing with interference characteristics of increasing the size of the body in combination with the 45° sweptback wing. These two groups of tests which are reported herein were conducted at Mach numbers from 0.6 to 1.13 at angles of attack of 0°, 2°, 4°, and 7° in the Langley 8-foot transonic tunnel.

The effect of longitudinal position of the wing on a body has been investigated and reported for another configuration in reference 3. These results are not included herein however, because a direct comparison of the two sets of data could not be made. The bodies used and the wing positions tested in the two investigations were different. In the present investigation the wing was moved forward instead of rearward as was the case for the investigation reported in reference 3.

In the present report, particular attention will be given the effects of wing-body interference on the aerodynamic characteristics of the wing in the transonic Mach number range, since references 1 and 2 indicate these effects are most pronounced in this speed range.

SYMBOLS

C_D drag coefficient, D/qS

C_L lift coefficient, L/qS

$\left(\frac{\partial C_L}{\partial \alpha}\right)_{av}$ average lift-curve slope for test angle-of-attack range

C_m pitching-moment coefficient, $\frac{M_{\bar{c}/4}}{qS\bar{c}}$

$\left(\frac{\partial C_m}{\partial C_L}\right)_{av}$ average slope for static longitudinal stability curve for test angle-of-attack range

c wing chord

$\bar{c}$ wing mean aerodynamic chord

D drag

d_{max}	maximum body diameter
L	lift
l	body length
M	Mach number
$M_{\bar{c}/4}$	pitching moment about $0.25\bar{c}$
q	dynamic pressure, $\frac{\rho V^2}{2}$
R	Reynolds number, based on $\bar{c}$
r	body radius at station x
S	wing area
V	free-stream velocity
x	longitudinal distance from nose of body
α	angle of attack
ρ	free-stream density

CONFIGURATIONS AND METHODS

Models

The wing of this investigation had 45° of sweepback of the 0.25 chord line, aspect ratio 4, taper ratio 0.6, and NACA 65A006 airfoil sections parallel to the plane of symmetry and has been described in reference 4. This wing was mounted in a midwing position on bodies developed from the basic body of revolution as shown in reference 2. The wing constructed of aluminum was tested in forward and rearward positions on a body characterized by a curved forebody, cylindrical midsection, and curved afterbody and has been completely described as body B in reference 2. The ordinates of this body are given in table I. The $\bar{c}/4$ for the wing in the rearward position was in the plane of the after limit of the cylindrical midsection, 26.67 inches from the nose of the body. The wing in the forward position was located 4 inches forward of the rearward wing position. (See fig. 1.) The ratio of the maximum cross-sectional area of the body to wing plan-form area was 0.0606 to 1.

The 45° sweptback wing also was tested in combination with two different body sizes (see fig. 2) which are referred to as the large and small bodies. The same aluminum wing employed in the investigation of the forward and rearward wing positions was used with the small body. A steel wing, identical in all other respects to the aluminum wing, was used with the large body. The small body had a curved forebody and a cylindrical afterbody which extended from a position just ahead of the leading edge of the wing rearward to the base of the model. This body has been completely described as body D in reference 2. The ordinates of this body are given in table I. The large body also had a curved forebody and a cylindrical afterbody. The diameter of the large body was 1.125 times greater than for the small body and the forebody shape was the same as for the small body. This large body has been completely described in reference 1; the ordinates are given in table I. The quarter chord of the mean aerodynamic chord of the wing was located at approximately the same percent of body length as for the small body. The ratio of the maximum cross-sectional area of the large body to wing area was 0.0767 to 1.

The surface of the model was maintained in a smooth condition throughout the investigation. Details of the location of the model in the tunnel are presented in figure 3. The models were sting-supported in the manner shown in figure 3 and described in reference 2. Figure 4 shows two photographs of the model installed in the test section.

Measurements

Forces and moments were measured by means of electrical strain-gage type of balances. The accuracy of the wing with interference data obtained from the strain-gage measurements of the various models tested is shown in table II.

Angles of attack were measured with the use of a cathetometer and an electrical strain-gage unit mounted in the nose of the model (see ref. 5) and are considered correct to within ±0.1°.

The static pressure at the rear of the models was obtained from pressure orifices located in the top and bottom of the sting support in the plane of the model base. All data presented have been adjusted for model base drag, the coefficients having been adjusted to a condition at which the base pressure is equal to the free-stream static pressure; therefore, the results do not include drag due to the base of the model.

RESULTS AND DISCUSSION

Presentation of Results

The average Reynolds number for these tests covered the range from 1.75×10^6 to 2.11×10^6 as shown in figure 5. These values are based on a mean aerodynamic chord length of 6.125 inches. The data herein are presented in terms of the wing with wing-body interference. These data were obtained by subtracting the body-alone data from similar wing-body-combination data and include the interference effect of the wing on the body as well as the interference effect of the body on the wing.

The axial development of cross-sectional area for the components and combinations used in the investigation of the wing in the forward and rearward positions on the body is shown in figure 6. The wing with interference data for the investigation of the wing in the forward and rearward positions are presented in figures 7(a), 7(b), and 7(c) in the form of angle of attack, drag coefficient, and pitching-moment coefficient against lift coefficient, respectively. Data for the wing in the rearward position and data for the body alone previously have been reported in reference 2. The analysis plots for the forward and rearward wing positions are shown as figures 8 to 11.

The wing with interference data for the investigation involving the two different body sizes are presented in figure 12. The results for the wing on the small body and for the small body alone have been presented in reference 2. The results for the wing on the large body are shown in reference 6 and the results for the large body alone may be found in reference 5. Analysis plots of the aerodynamic characteristics of the wing with interference from the two bodies are presented as figures 13 to 16.

Effect of Wing Location

Lift.- The variation of the average lift-curve slope with Mach number, as shown in figure 8, indicates that, within the accuracy of the tests, the lift results were essentially the same for the wing in the forward and rearward positions on the body.

Drag.- The most dominant feature of locating the sweptback wing forward on the body was the reduction of the adverse drag rise which occurs up to a Mach number of 1.00 for lift coefficients up to 0.4 (fig. 9). The drag rise is defined as that increase in drag which occurs with the onset of shock formation and associated flow separation as Mach number is increased. The drag rise for the wing forward was 15 percent less than for the wing rearward at a lift coefficient of 0, and 30 percent less at

a lift coefficient of 0.2. These reductions might be expected on the basis of the less rapid rate of change of cross-sectional area over the rear portion of the combination with the wing forward as compared with that for the combination with the wing rearward. (See fig. 6.) As pointed out in reference 1, a reduction in rate of change in cross sectional area of a particular configuration results in reduced induced velocities and adverse gradients which lead to weaker drag-producing shocks in the field of flow of the configuration. At Mach numbers above 1.05 the total drag rise for the two cases appears to be the same within the accuracy of the investigation.

The decrease in zero-lift drag coefficient associated with the wing forward at subsonic Mach numbers is identical to the trend shown by the comparison of the drag coefficients for the wing in the presence of bodies A and B in reference 2. In this reference, it is shown that, at a lift coefficient of zero, the absolute drag of the wing nearer the nose of the body was the lesser, as in the present case. This agreement suggests that the drag differences are due to the relation of the wing to the forebody. At the lifting conditions, the values of drag coefficient are shown to be slightly higher for the forward wing at subsonic speeds.

A comparison of the maximum lift-drag ratios for the two configurations (fig. 10) indicates that, in the subsonic range up to a Mach number of 0.95, higher values were obtained for the wing rearward. In the transonic range the maximum lift-drag ratios for the two configurations are about the same. The lift coefficient for maximum lift-drag ratio was less for the wing forward than for the wing rearward throughout the test Mach number range.

Pitching moment.- The variation of pitching-moment coefficient with lift coefficient appears to be more linear for the wing in the forward position than rearward for Mach numbers from 0.90 to 1.13 (fig. 7(c)). The interference effect of forward and rearward wing position on the aerodynamic-center location referred to $\bar{c}/4$ (positive values of average $\partial C_m/\partial C_L$ forward of $\bar{c}/4$) is shown in figure 11. The trend of aerodynamic-center location with Mach number for the two cases is essentially the same. (See fig. 11.)

It is believed that the pitch-up characteristics of the wing with interference should not be significantly altered by the change in longitudinal location of the wing. Pitching-moment results presented in reference 2 serve as a basis for this assumption. In reference 2, it is shown that a change in body length equivalent to moving the leading edge of the wing 6.67 inches nearer the nose of the body had little effect on the pitch-up characteristics of the wing with interference.

Effect of Body Size

An examination of the results presented in reference 7 leads to the conclusion that any differences in bending between the aluminum and steel wings of this investigation would not have any effect on the lift and drag characteristics of the wing with interference up to the highest angle of attack, 7°, tested. It is indicated also that the pitching-moment characteristics of the wing with interference would be affected because of the difference in amount of twist between the aluminum and steel wings under load.

Lift.- The most noticeable effect of increasing the size of the body was the increase in average lift-curve slope of the wing with interference as shown in figure 13. The higher average lift-curve slope for the larger body may be attributed directly to the greater amount of upflow associated with the larger body. This upflow produced greater lift over the inboard portions of the wing in the presence of the large body.

Drag.- The most interesting effect of increasing the body size on the drag characteristics of the wing with interference is the marked reduction in drag rise at zero lift in the transonic range (fig. 14). At a lift coefficient of 0 and in the transonic range, the drag rise was from 30 to 50 percent less than for the wing with interference from the small body. Further discussion of this phenomenon will be delayed until additional evidence can be obtained to substantiate the present results. The drag for the lifting conditions was greater for the large body configuration. As a result, the maximum lift-drag ratio for the wing in the presence of the large body was less than for the small body configuration throughout the Mach number range of the investigation (fig. 15). The lift coefficient for maximum lift-drag ratio remained approximately the same for the wing in the presence of either the large or small body.

Pitching moment.- The values of the average slope for the static longitudinal stability curve are shown in figure 16 to be more positive for the wing with interference for the small body test than for the large body. This result, however, cannot be attributed to a difference in body size but more to a difference in the material used in the construction of the wing for the two cases. On the basis of the results reported in reference 7, it is concluded that the difference in average slope for the static longitudinal stability curve is due primarily to the greater degree of twist of the aluminum wing tested in conjunction with the small body than to the steel wing used on the large body. The difference between the $(\partial C_m/\partial C_L)_{av}$ values throughout the Mach number range for the two wings in the present investigation is the same as that

shown for $\partial C_m/\partial C_L$ at $C_L = 0$ and 0.4 for the two wings investigated and reported in reference 7. The variation with Mach number was practically the same for the two investigations.

A comparison of the pitching-moment data for the two wing-body combinations involving the wing on the small body (body D with configuration D in ref. 2) and the wing on the large body (wing with cylindrical body in ref. 6) indicates that the increase in body size had no effect on the pitch-up characteristics of the combination. On this basis, the pitch-up characteristics for the wing with interference of the present investigation may be considered to be the same for both bodies tested.

CONCLUSIONS

A transonic wind-tunnel investigation of the characteristics of a 45° sweptback wing in two longitudinal locations on a body and for the same wing on two bodies of varying size indicated the following conclusions:

1. The zero-lift drag coefficient of the wing forward with interference was considerably lower throughout the Mach number range than that of the wing rearward with interference. A reduction in the transonic drag rise of the wing with interference was obtained up to a Mach number of approximately 1.00 for the wing in the forward position compared with the rearward position at lift coefficients up to 0.4. At the test Mach numbers above 1.05, little or no difference in the magnitude of the drag rise was noted for the two cases.

2. The variations of lift-curve slope and aerodynamic-center location with Mach number were little affected by a change in location of the wing on the body.

3. The average lift-curve slope for the wing with interference from the large body was greater than for the wing with interference from the small body throughout the Mach number range.

4. The drag rise for the wing with interference from the large body at nonlifting conditions was 30 to 50 percent less than for the wing with interference from the small body in the transonic-speed range.

5. The pitching-moment characteristics of the wing with interference were not severely affected by a change in body size.

Langley Aeronautical Laboratory,
National Advisory Committee for Aeronautics,
Langley Field, Va.

REFERENCES

1. Whitcomb, Richard T.: A Study of the Zero-Lift Drag-Rise Characteristics of Wing-Body Combinations Near the Speed of Sound. NACA RM L52H08, 1952.

2. Loving, Donald L., and Wornom, Dewey E.: Transonic Wind-Tunnel Investigation of the Interference Between a 45° Sweptback Wing and a Systematic Series of Four Bodies. NACA RM L52J01, 1952.

3. Hallissy, Joseph M., and Bowman, Donald R.: Transonic Characteristics of a 45° Sweptback Wing-Fuselage Combination. Effect of Longitudinal Wing Position and Division of Wing and Fuselage Forces and Moments. NACA RM L52K04, 1952.

4. Osborne, Robert S.: A Transonic-Wing Investigation in the Langley 8-Foot High-Speed Tunnel at High Subsonic Mach Numbers and at a Mach Number of 1.2. Wing-Fuselage Configuration Having a Wing of 45° Sweepback, Aspect Ratio 4, Taper Ratio 0.6, and NACA 65A006 Airfoil Section. NACA RM L50H08, 1950.

5. Williams, Claude V.: A Transonic Wind-Tunnel Investigation of the Effects of Body Indentation, as Specified by the Transonic Drag-Rise Rule, on the Aerodynamic Characteristics and Flow Phenomena of an Unswept-Wing–Body Combination. NACA RM L52L23, 1953.

6. Robinson, Harold L.: A Transonic Wind-Tunnel Investigation of the Effects of Body Indentation, as Specified by the Transonic Drag-Rise Rule, on the Aerodynamic Characteristics and Flow Phenomena of a 45° Sweptback-Wing–Body Combination. NACA RM L52L12, 1953.

7. Osborne, Robert S., and Mugler, John P., Jr.: Effects of Wing Elasticity on the Aerodynamic Characteristics of a 45° Sweptback-Wing–Fuselage Combination Measured in the Langley 8-Foot Transonic Tunnel. NACA RM L52G23, 1952.

TABLE I

ORDINATES AND DIMENSIONS OF BODIES USED IN INVESTIGATION

OF WING LOCATION AND BODY SIZE

Body used for wing location investigation

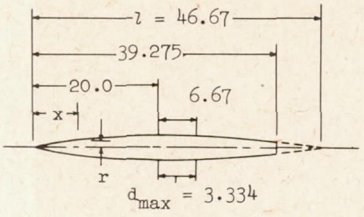

Small body

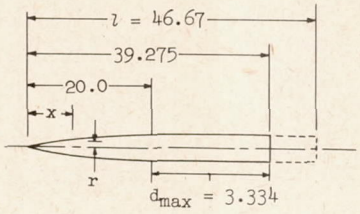

Large body

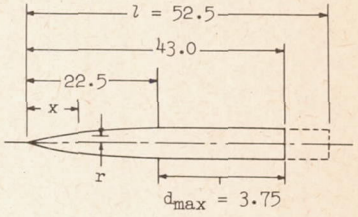

Body ordinates	
x/l	r/l
0	0
.0043	.00198
.0064	.00255
.0107	.00367
.0214	.00619
.0429	.01033
.0643	.01382
.0857	.01689
.1286	.02222
.1714	.02648
.2143	.02970
.2571	.03206
.3000	.03371
.3428	.03482
.3857	.03551
.4285	.03571
.4750	.03571
.5000	.03571
.5250	.03571
.5500	.03571
.5715	.03571
.6144	.03539
.6572	.03449
.7000	.03293
.7429	.03053
.7858	.02681
.8286	.02165
.8571	.01734
.8714	.01587
.9143	.00964
.9571	.00376
1.0000	0
L.E. radius = 0.0005	

Body ordinates	
x/l	r/l
0	0
.0043	.00198
.0064	.00255
.0107	.00367
.0214	.00619
.0429	.01033
.0643	.01382
.0857	.01689
.1286	.02222
.1714	.02648
.2143	.02970
.2571	.03206
.3000	.03371
.3428	.03482
.3857	.03551
.4285	.03571
.4750	.03571
.5000	.03571
.5250	.03571
.5500	.03571
.5715	.03571
.6144	.03571
.6572	.03571
.7000	.03571
.7429	.03571
.7858	.03571
.8286	.03571
.8571	.03571
.8714	.03571
.9143	.03571
.9571	.03571
1.0000	.03571
L.E. radius = 0.0005	

Body ordinates	
x/l	r/l
0	0
.0043	.00198
.0064	.00255
.0107	.00367
.0214	.00619
.0429	.01033
.0643	.01382
.0857	.01689
.1286	.02222
.1714	.02648
.2143	.02970
.2571	.03206
.3000	.03371
.3428	.03482
.3857	.03551
.4285	.03571
.4750	.03571
.5000	.03571
.5250	.03571
.5500	.03571
.5715	.03571
.6144	.03571
.6572	.03571
.7000	.03571
.7429	.03571
.7858	.03571
.8286	.03571
.8571	.03571
.8714	.03571
.9143	.03571
.9571	.03571
1.0000	.03571
L.E. radius = 0.0005	

TABLE II

ACCURACY OF WING WITH INTERFERENCE DATA FROM STRAIN-GAGE MEASUREMENTS

Coefficient	Aluminum wing forward, rearward, and on small body; $\alpha = 0^\circ, 2^\circ, 4^\circ$, and 7°		Steel wing on large body; $\alpha = 0^\circ, 2^\circ, 4^\circ$, and 7°	
	Mach number, 0.60	Mach number, 1.00	Mach number, 0.60	Mach number, 1.00
C_L	±0.008	±0.004	±0.016	±0.008
C_D	±.001	±.0005	±.002	±.001
C_m	±.005	±.003	±.003	±.002

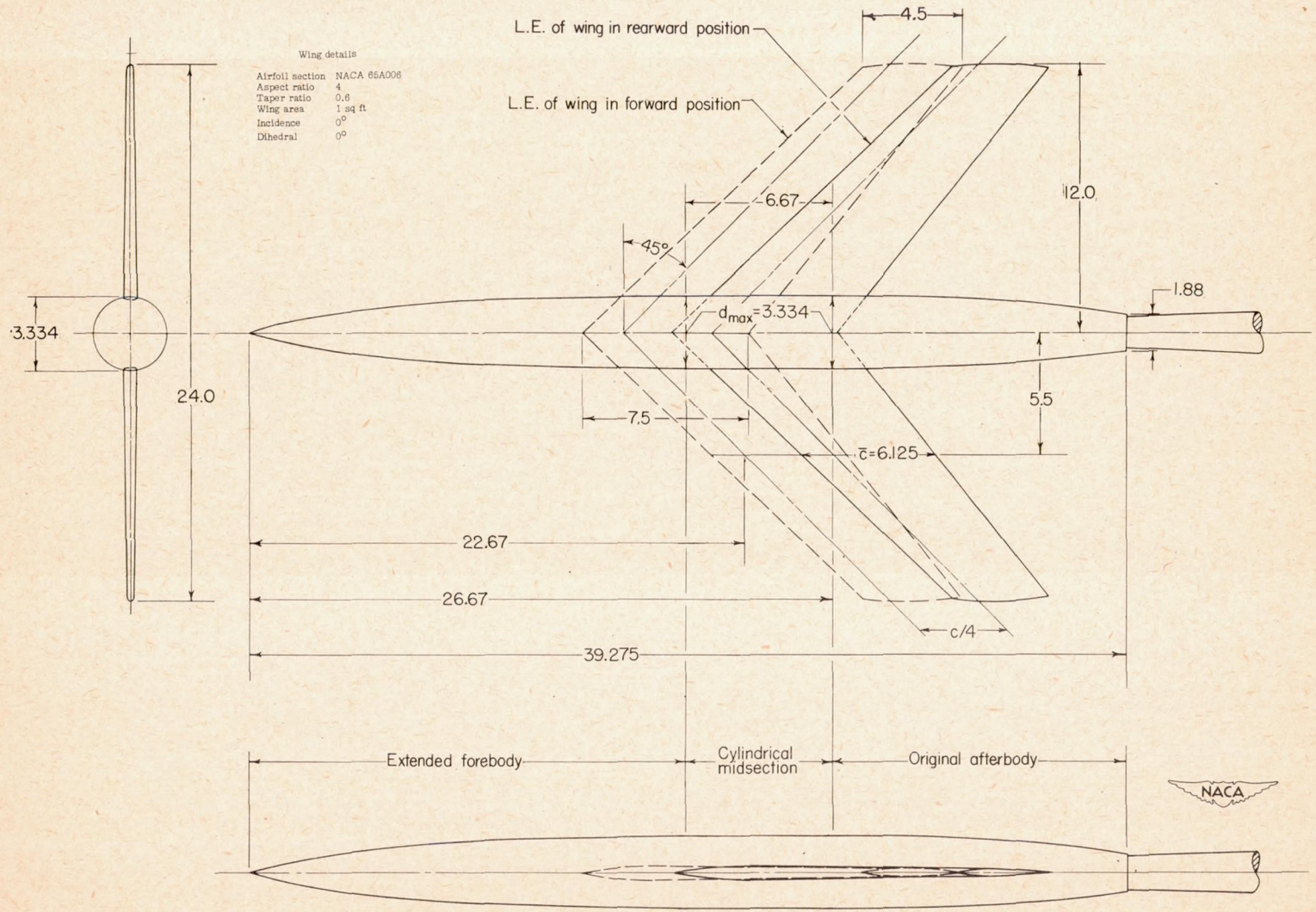

Figure 1.- Dimensions of models used for investigation of wing location on body. All linear dimensions are in inches.

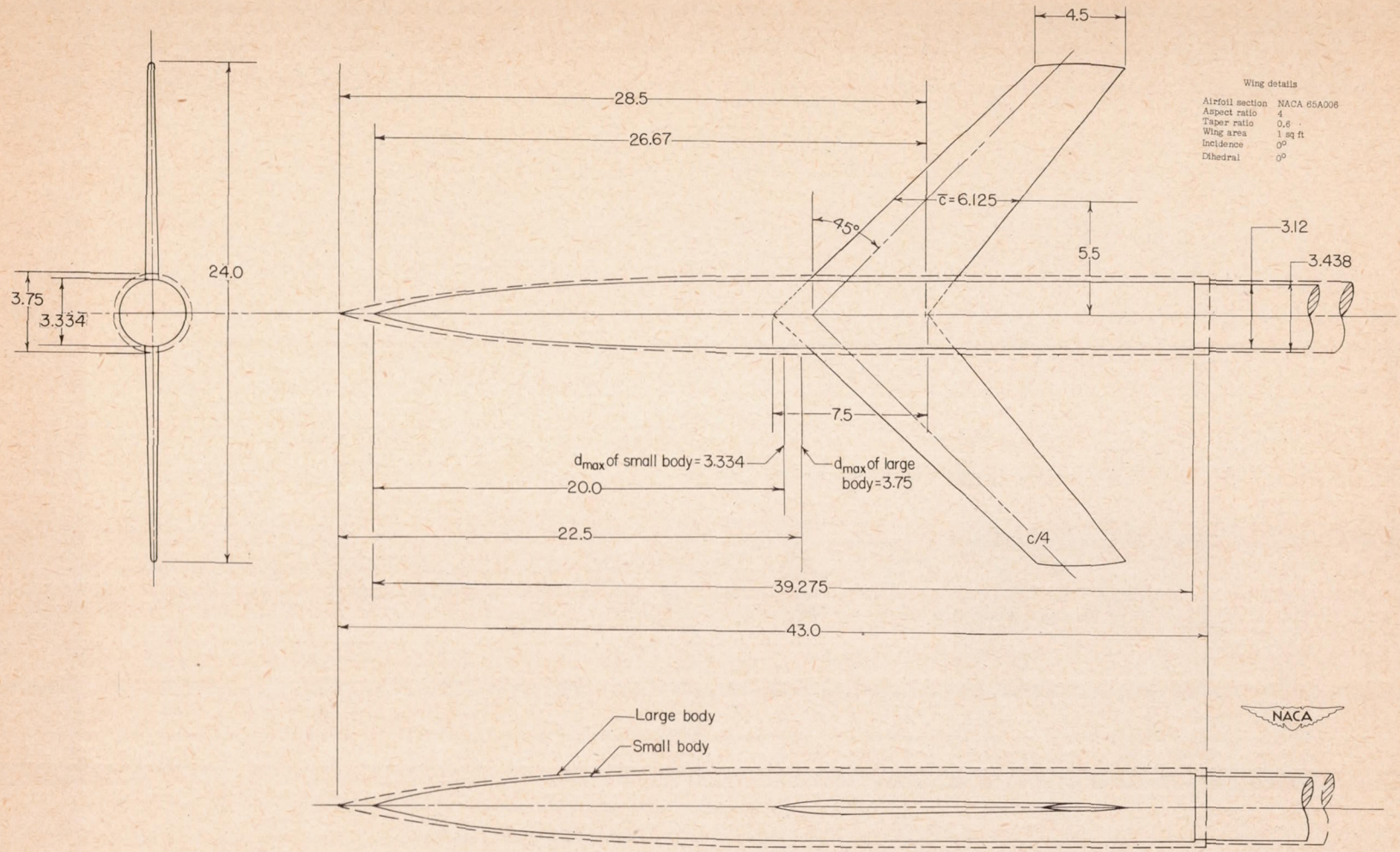

Figure 2.- Dimensions of models used for investigation of body size.
All linear dimensions are in inches.

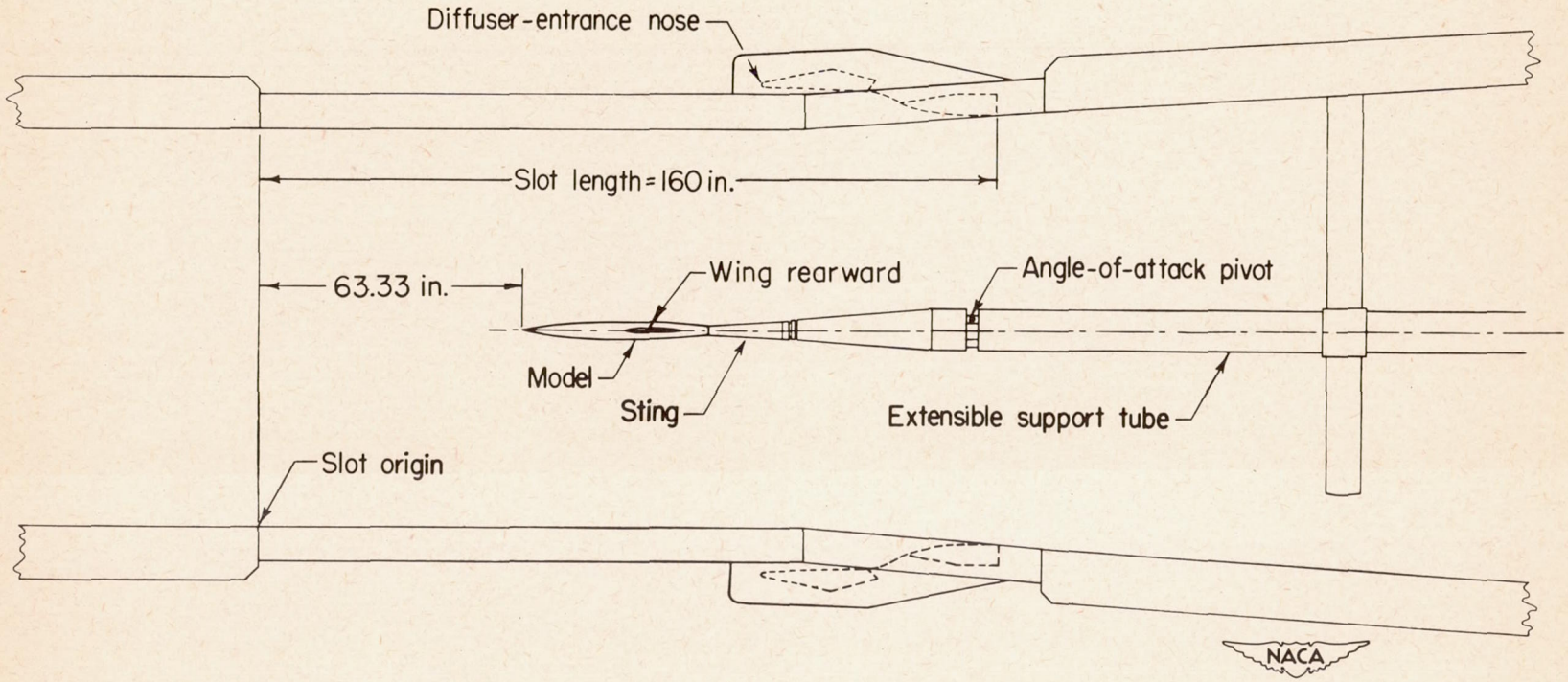

Figure 3.- Details of the typical location of the models in the slotted test section of the Langley 8-foot transonic tunnel.

CONFIDENTIAL

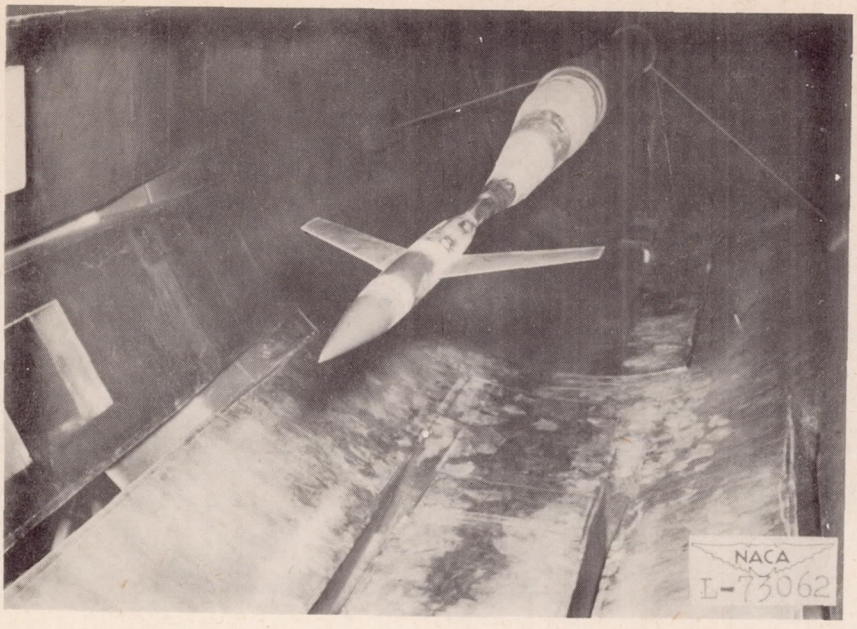

(a) Front view.

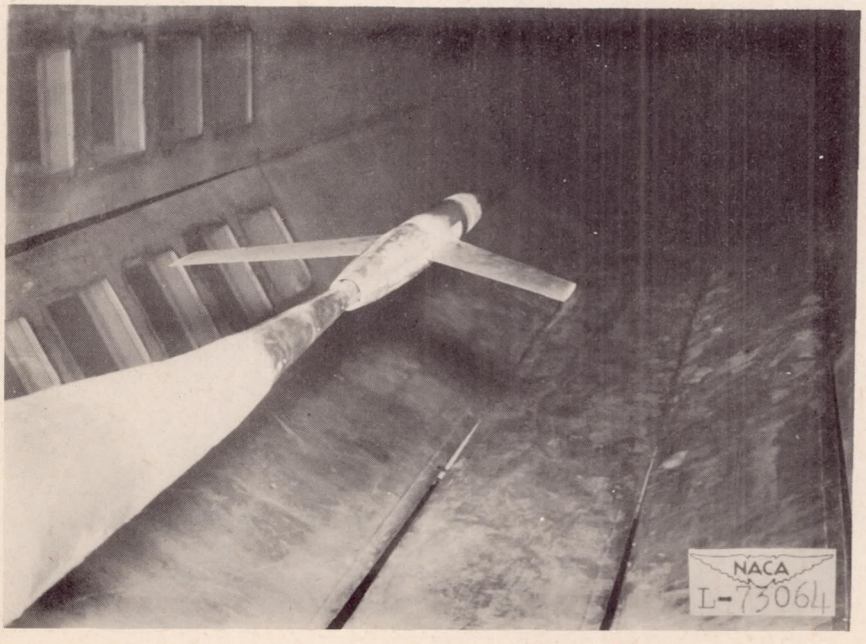

(b) Rear view.

Figure 4.- Wing-body combination with wing in rearward location in Langley 8-foot transonic tunnel.

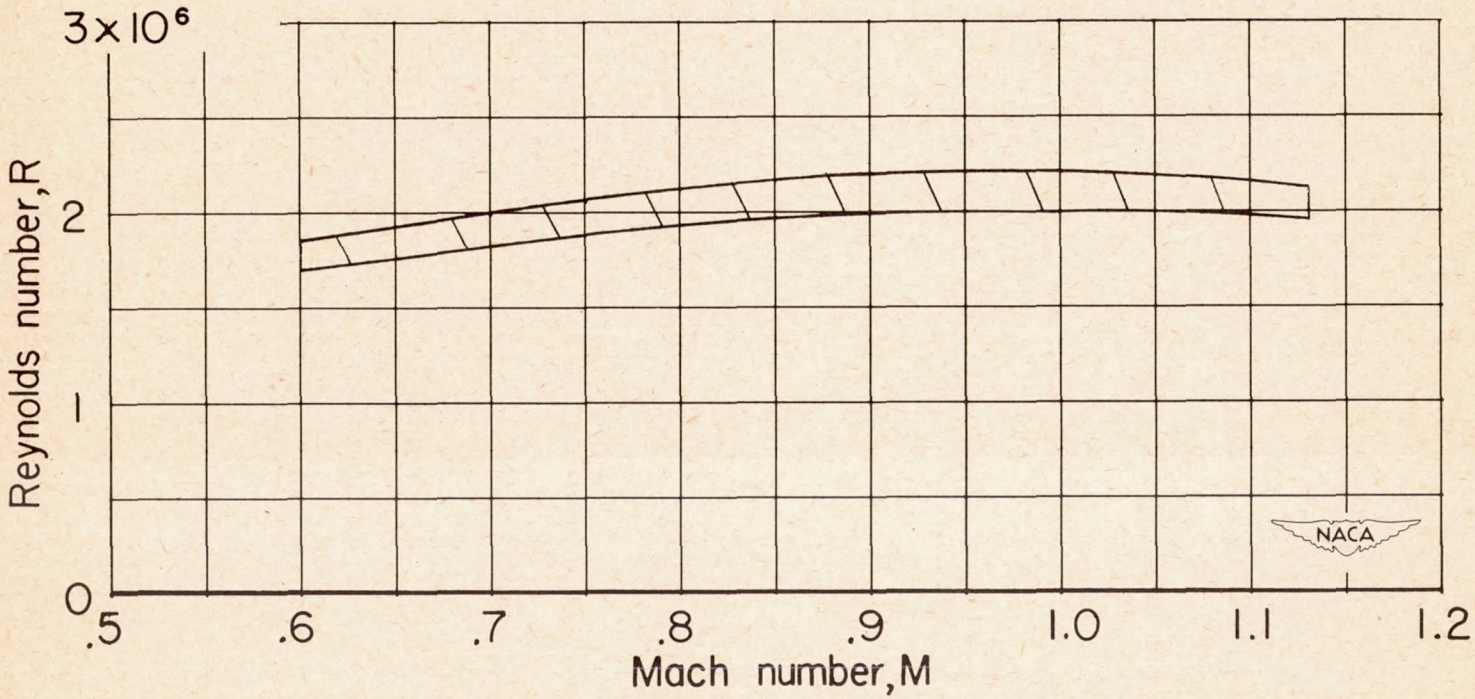

Figure 5.- Variation with Mach number of Reynolds number based on a mean aerodynamic chord length of 6.125 inches.

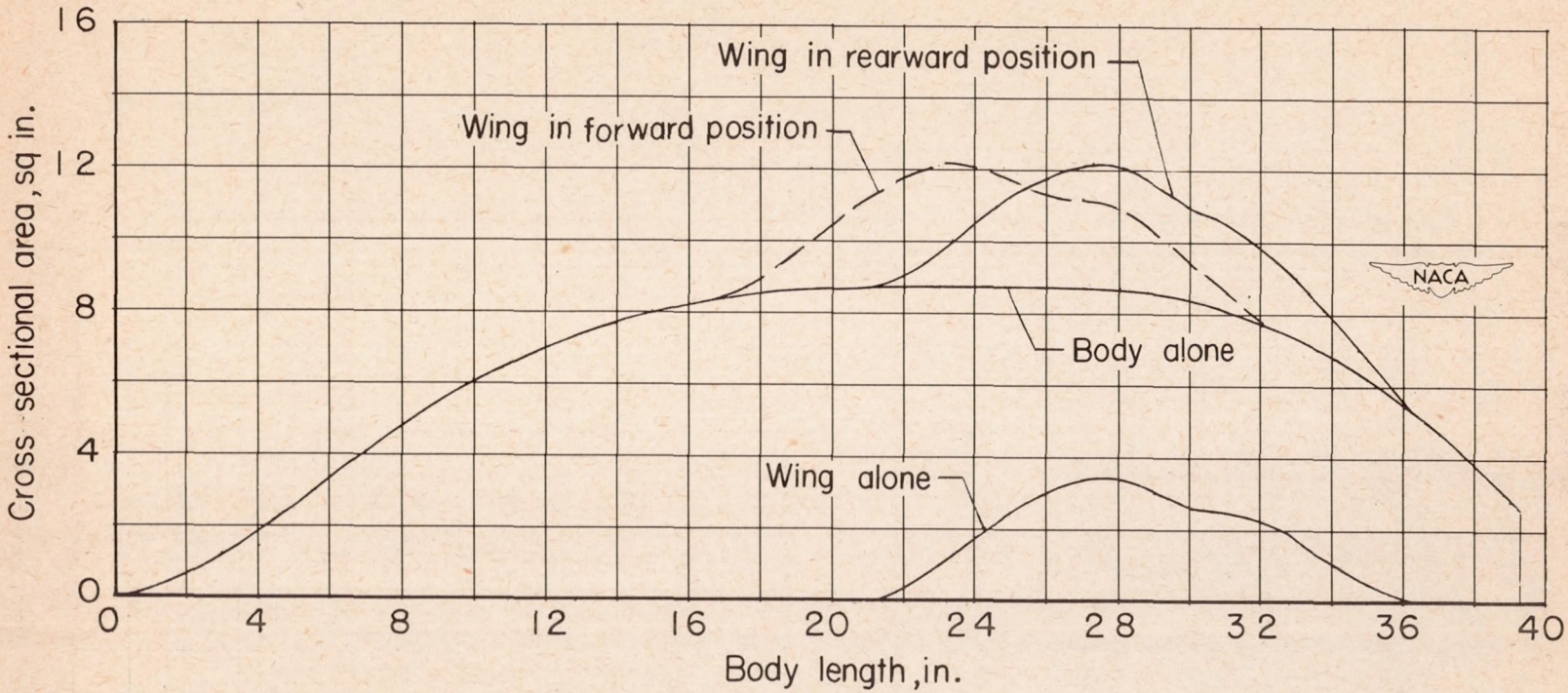

Figure 6.- Axial development of cross-sectional area for the various components and combinations used in the investigation of wing location.

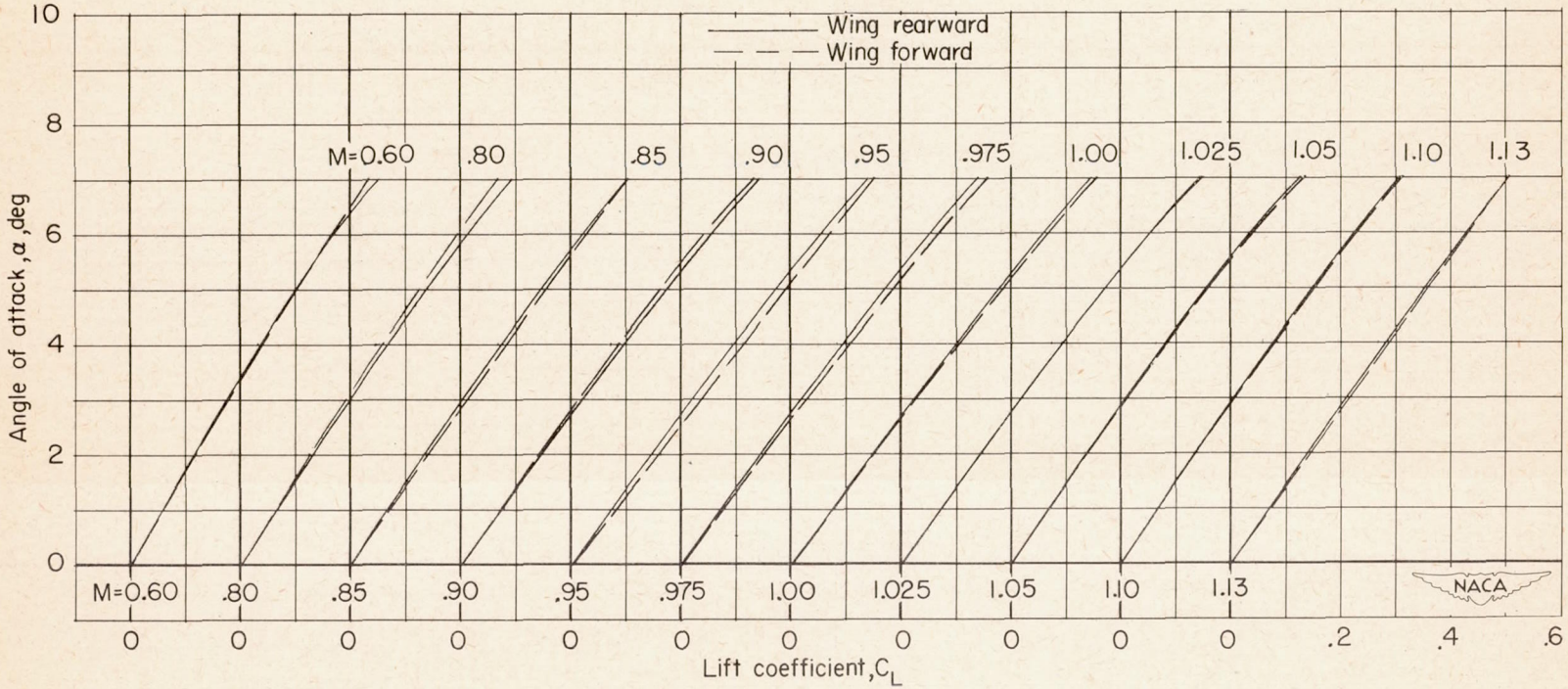

(a) α against C_L.

Figure 7.- Aerodynamic characteristics for the wing with interference for two longitudinal positions.

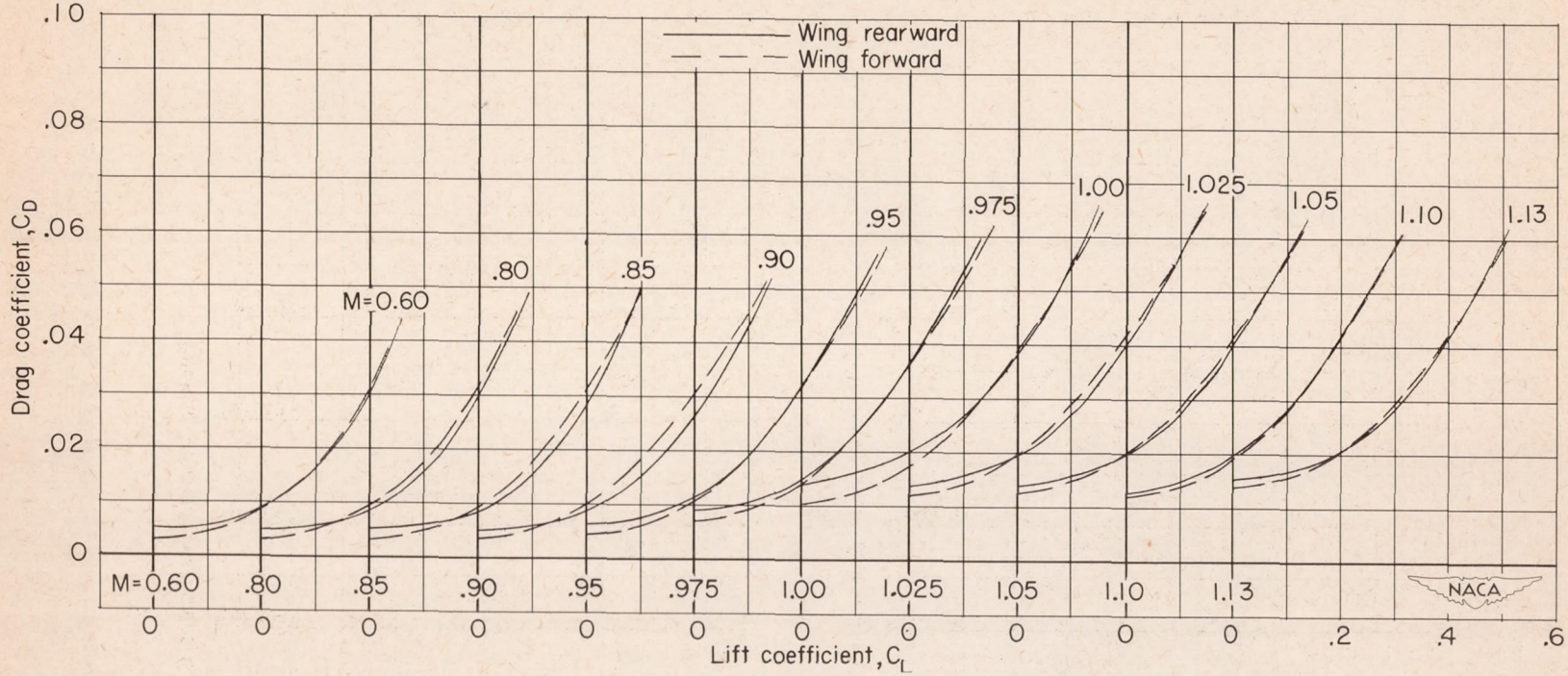

(b) C_D against C_L.

Figure 7.- Continued.

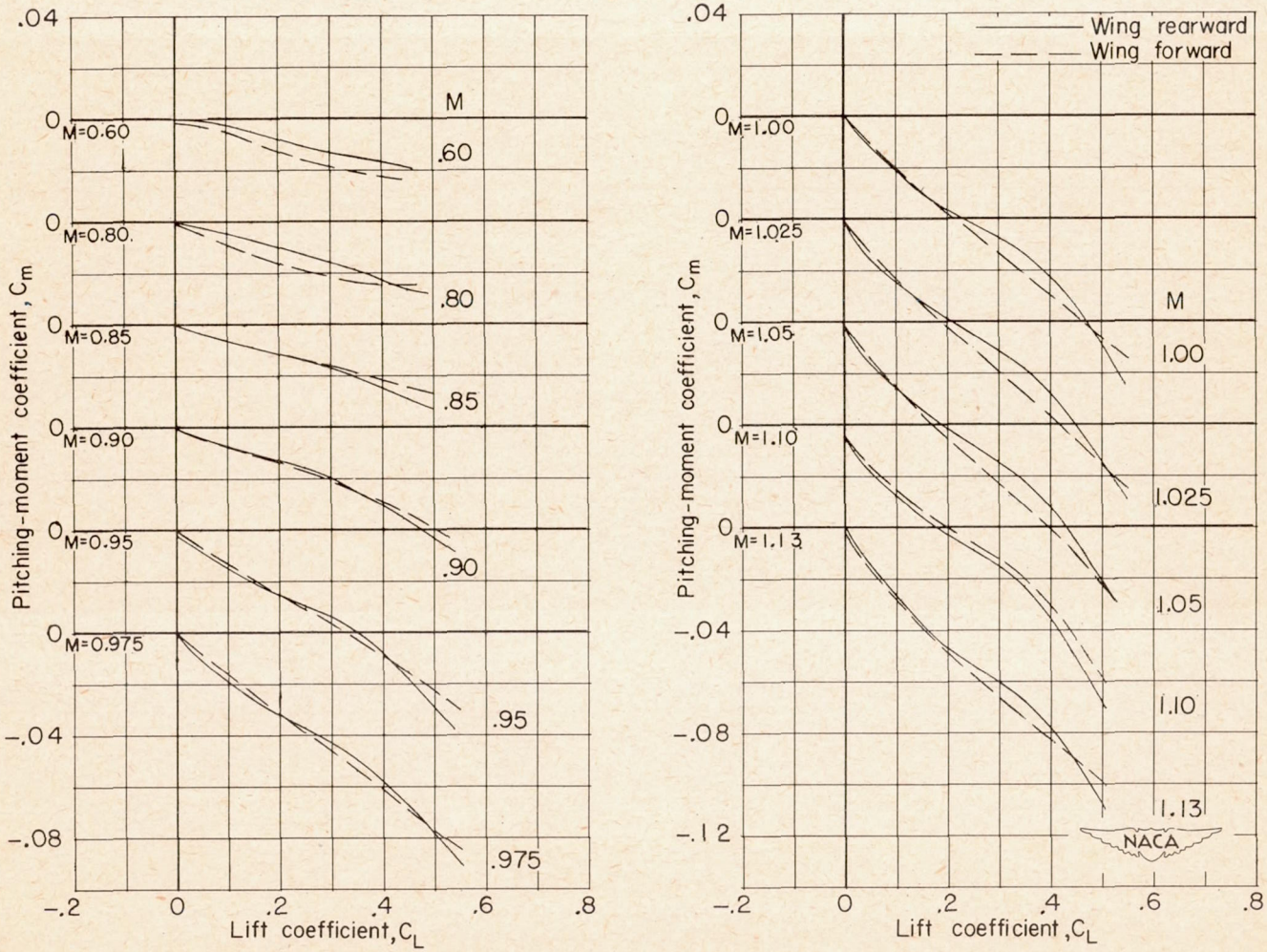

(c) C_m against C_L.

Figure 7.- Concluded.

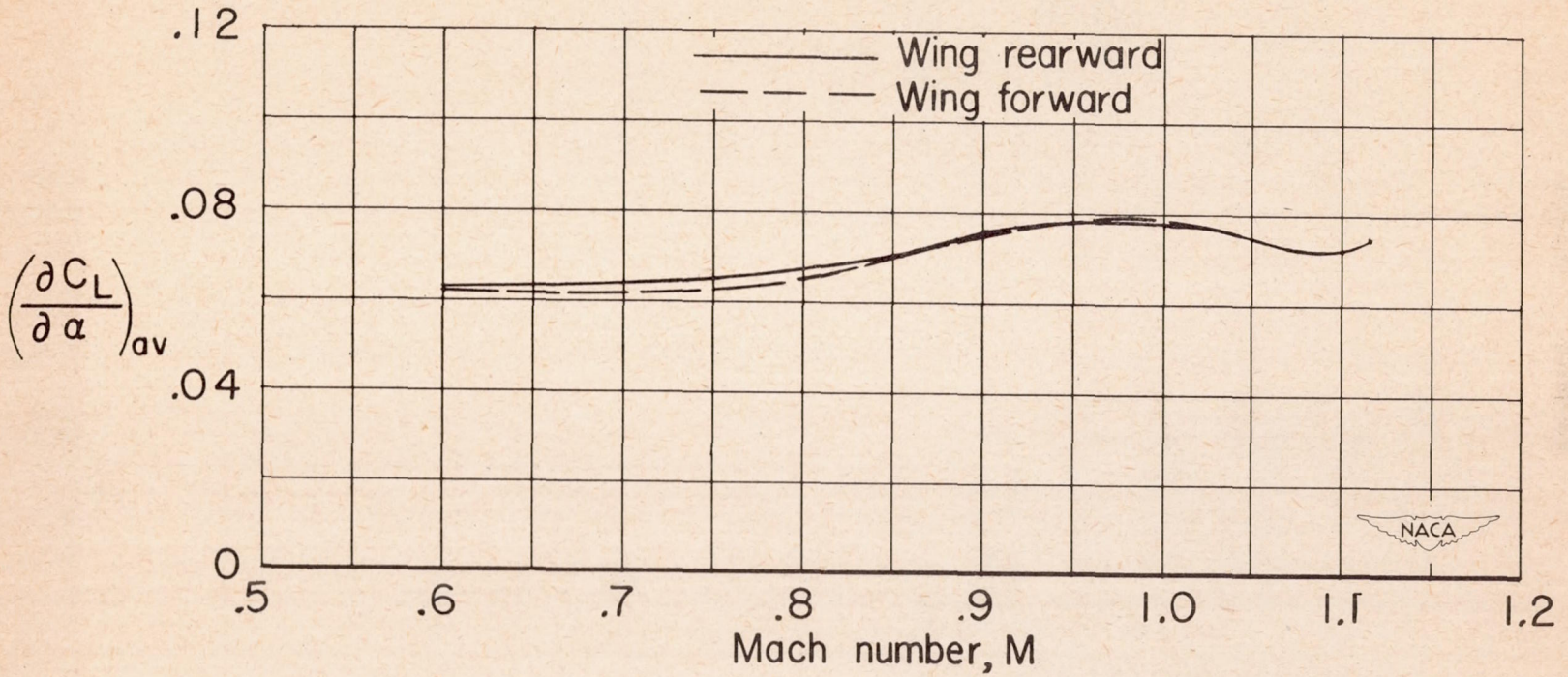

Figure 8.- Variation of average lift-curve slope with Mach number for the wing with interference for two longitudinal positions.

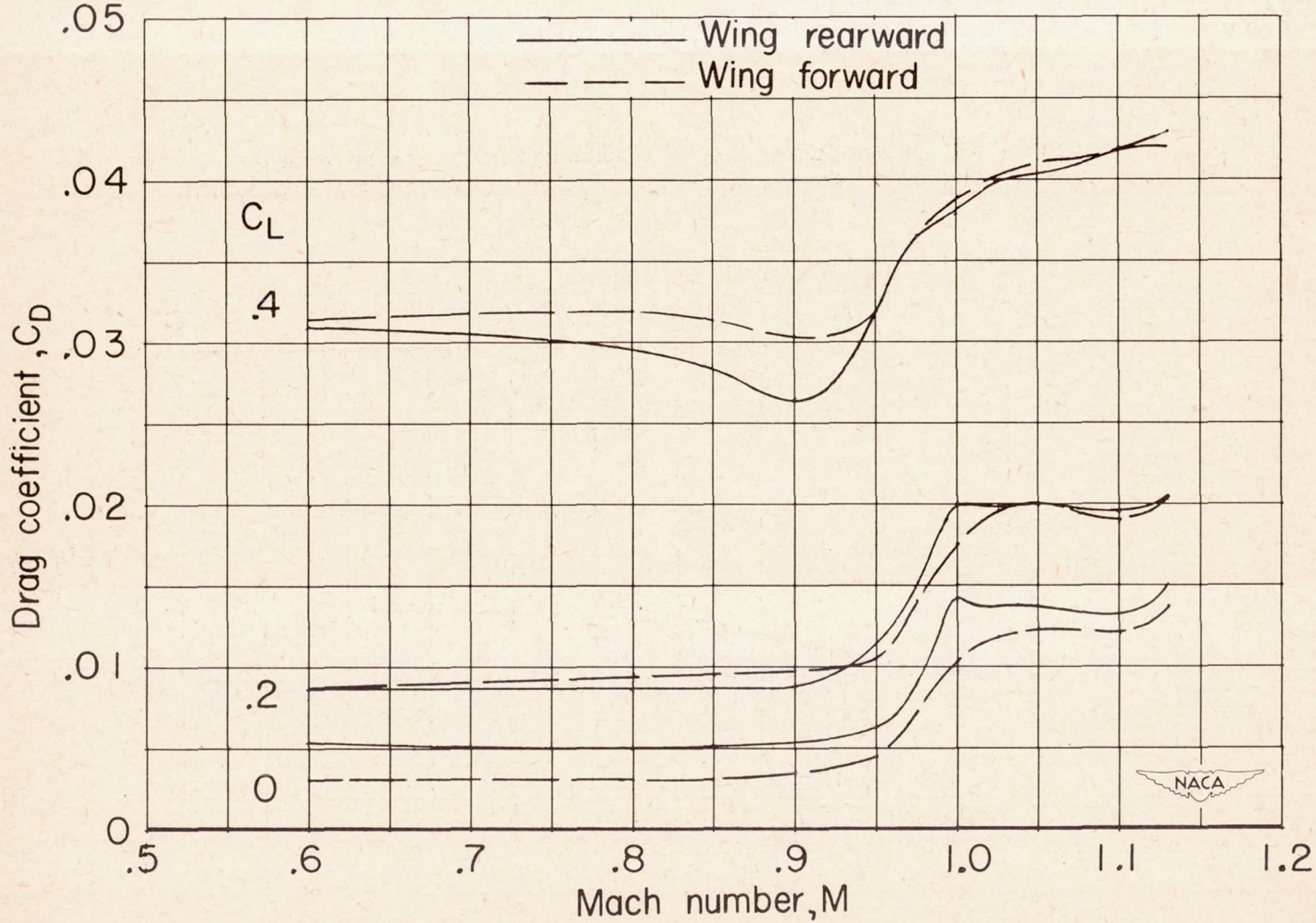

Figure 9.- Variation of drag coefficient with Mach number for the wing with interference for two longitudinal positions.

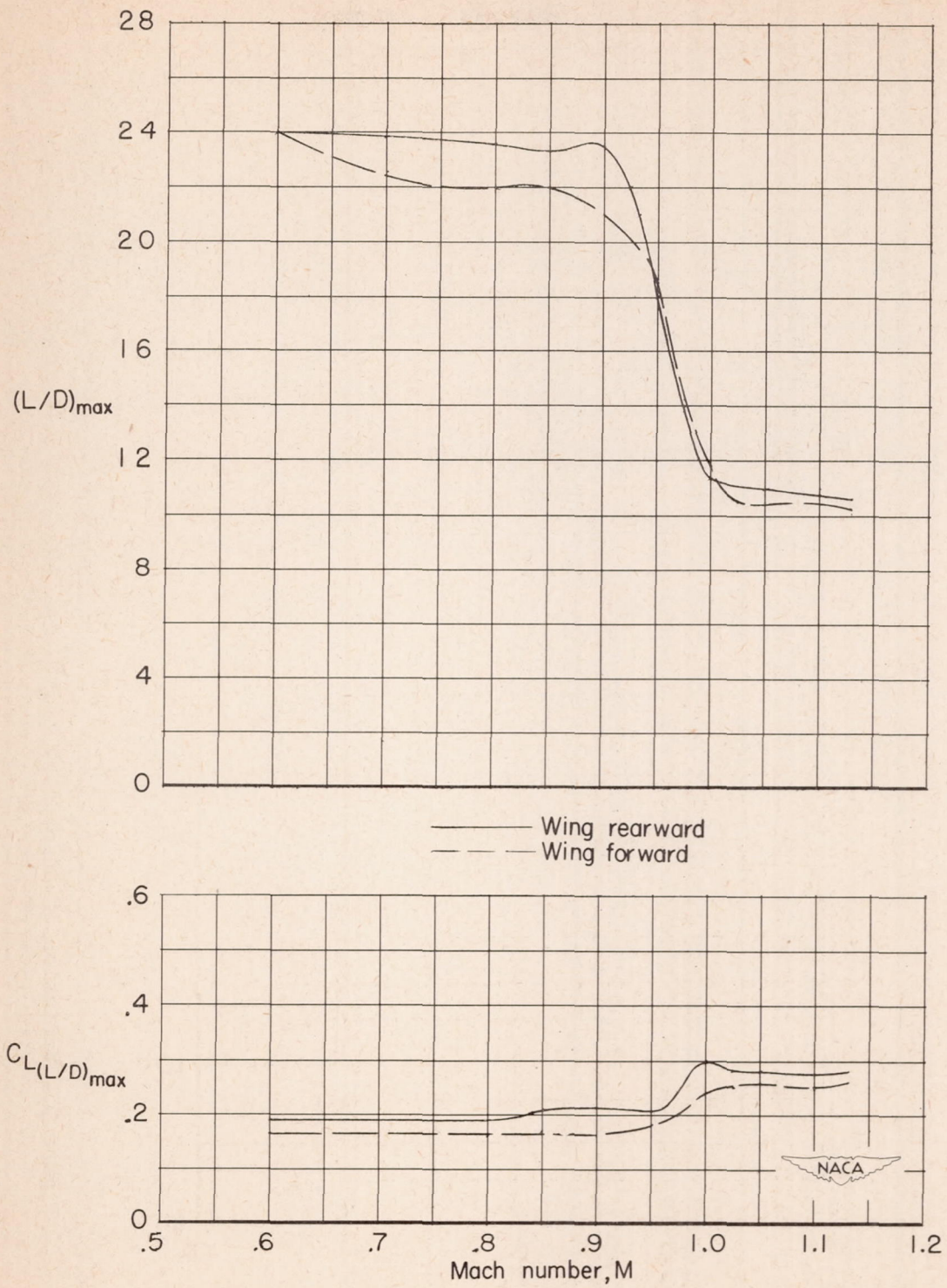

Figure 10.- Variation of maximum lift-drag ratio and lift coefficient for maximum lift-drag ratio with Mach number for the wing with interference for two longitudinal positions.

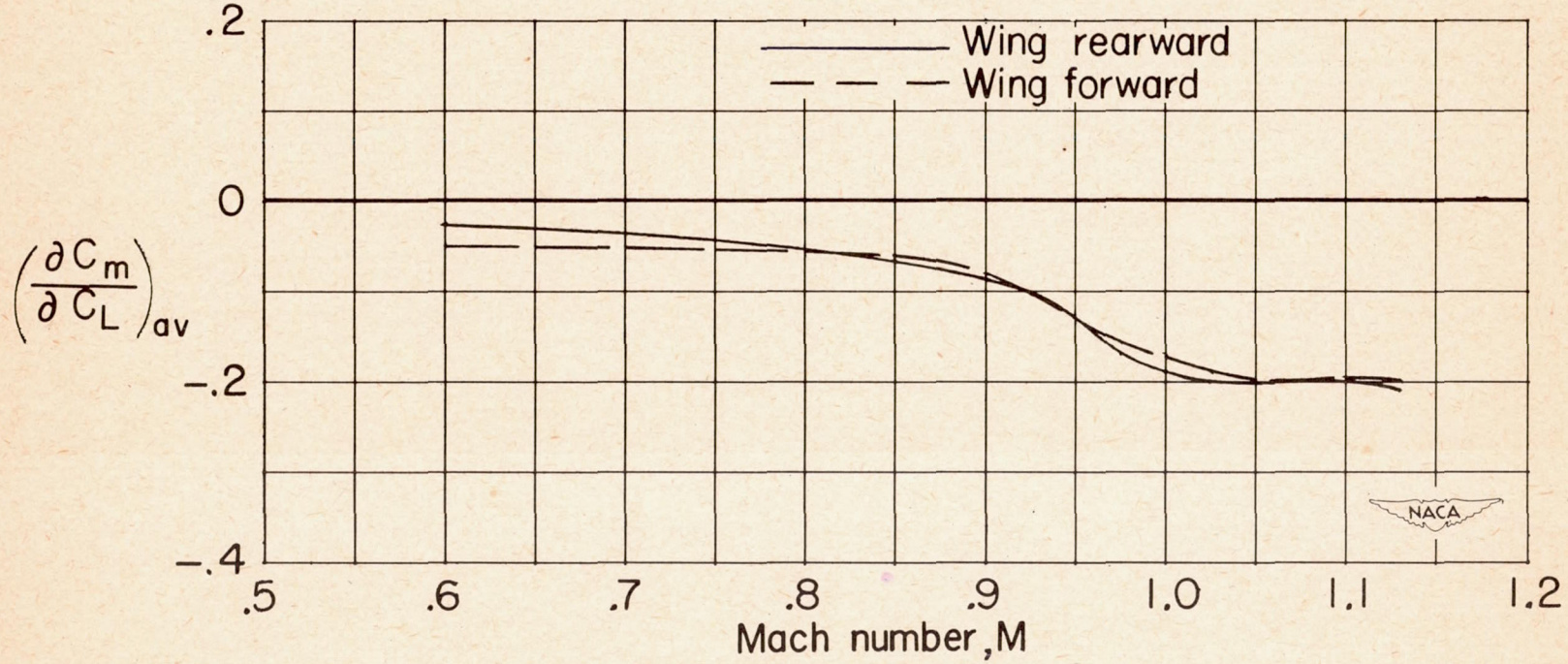

Figure 11.- Variation of average slope for the static longitudinal stability curve with Mach number for the wing with interference for two longitudinal positions.

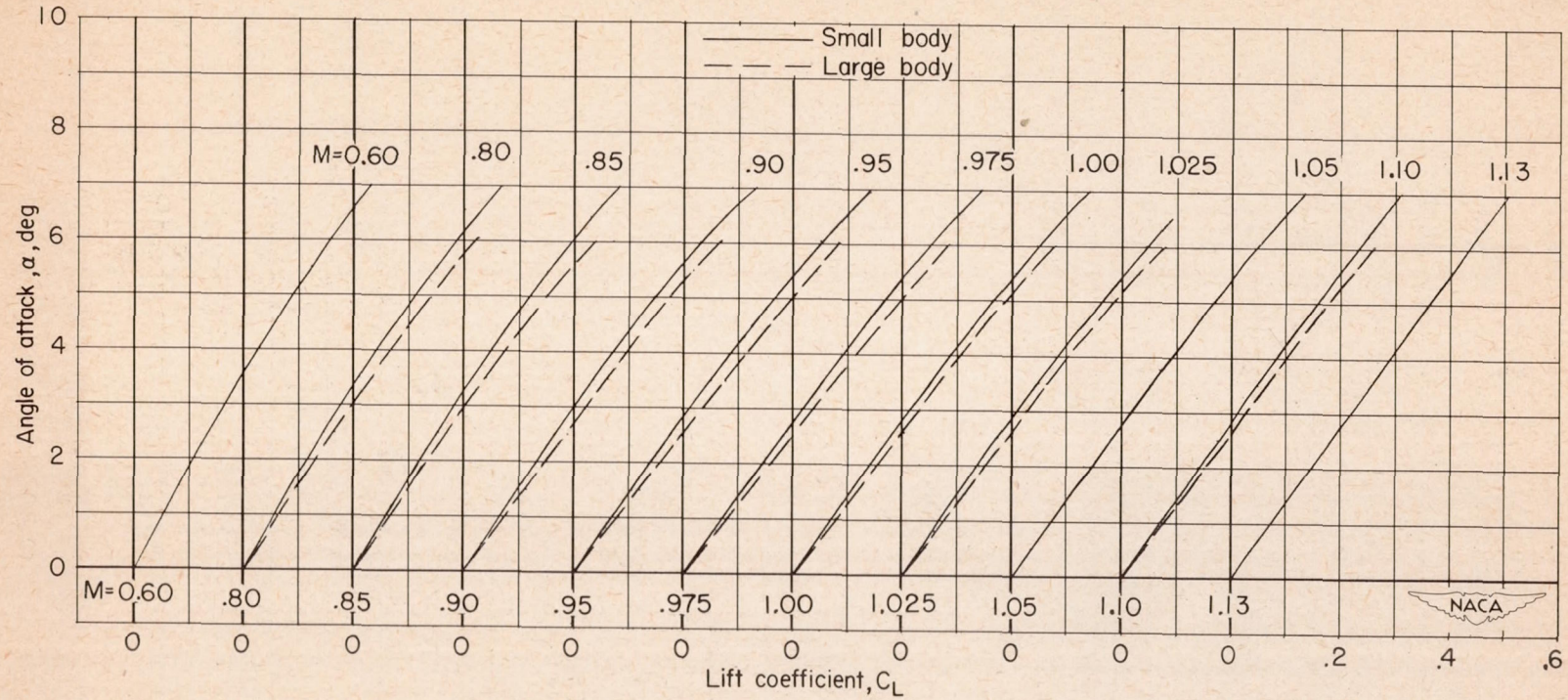

(a) α against C_L.

Figure 12.- Basic aerodynamic characteristics of the wing with interference when mounted on a small and a large body of similar shape.

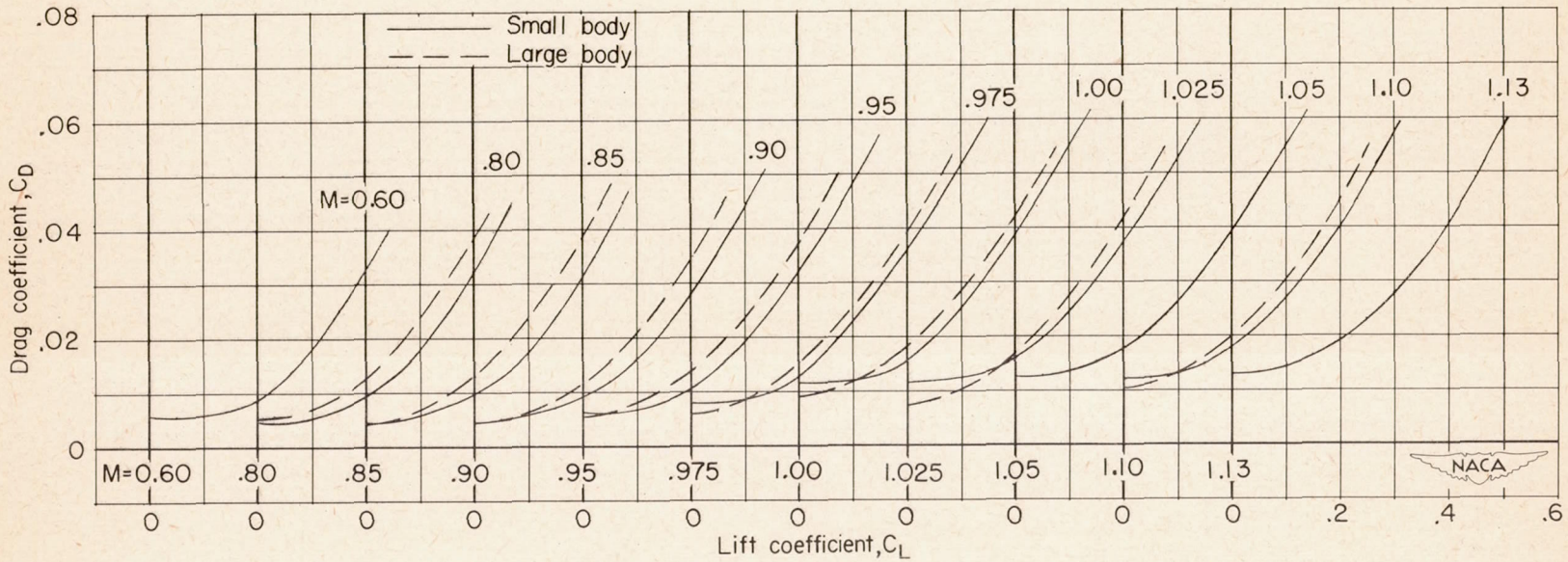

(b) C_D against C_L.

Figure 12.- Continued.

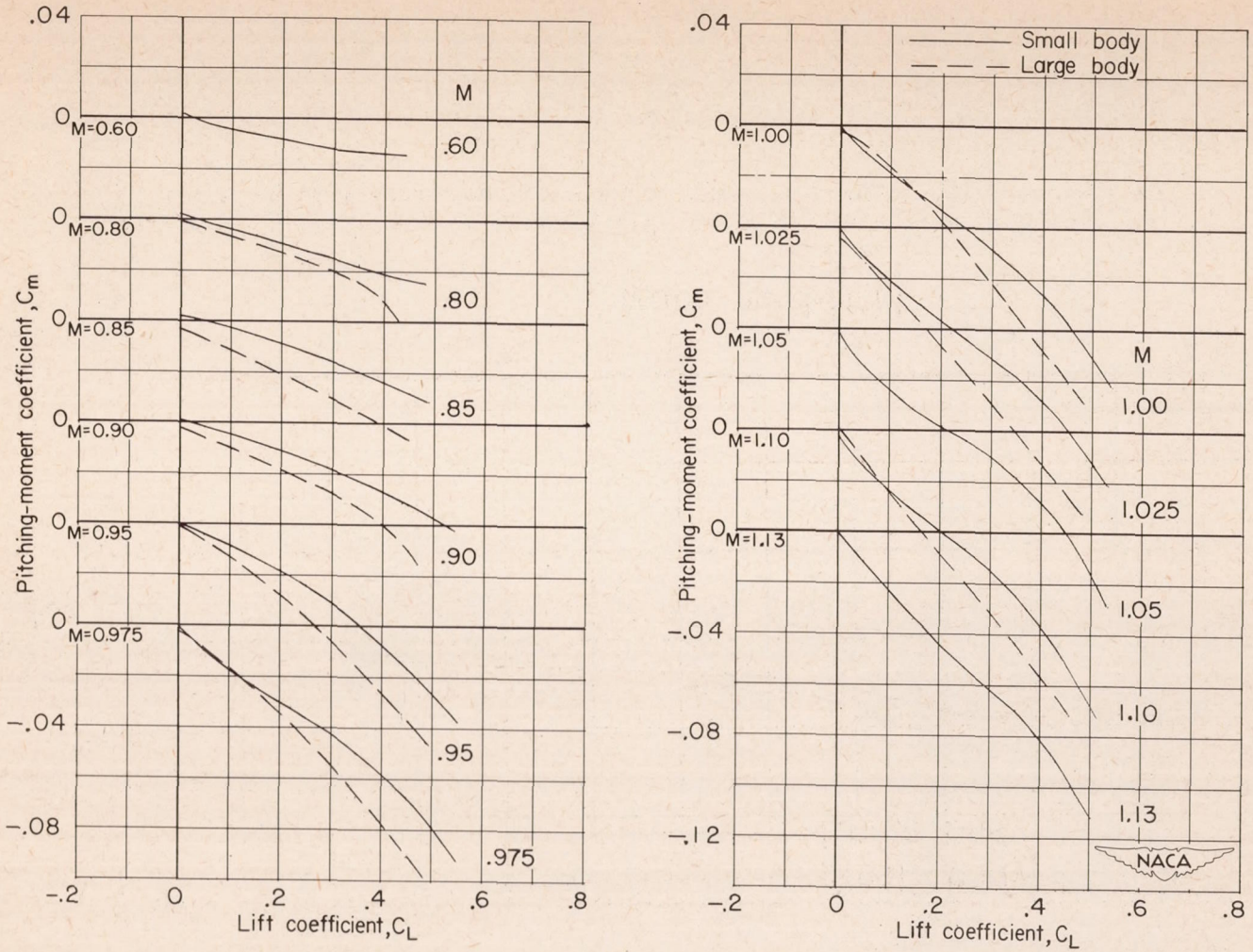

(c) C_m against C_L.

Figure 12.- Concluded.

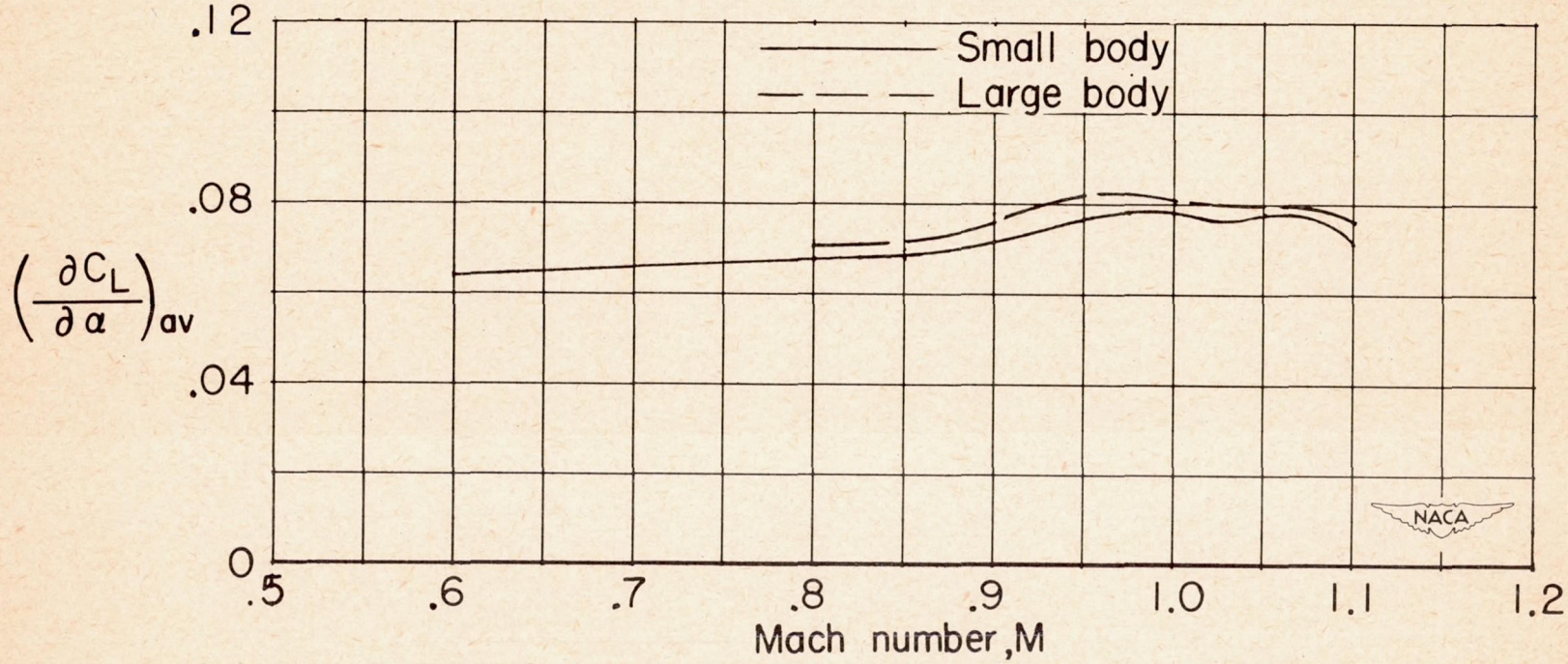

Figure 13.- Variation of average lift-curve slope with Mach number for the wing with interference when mounted on a small and a large body of similar shape.

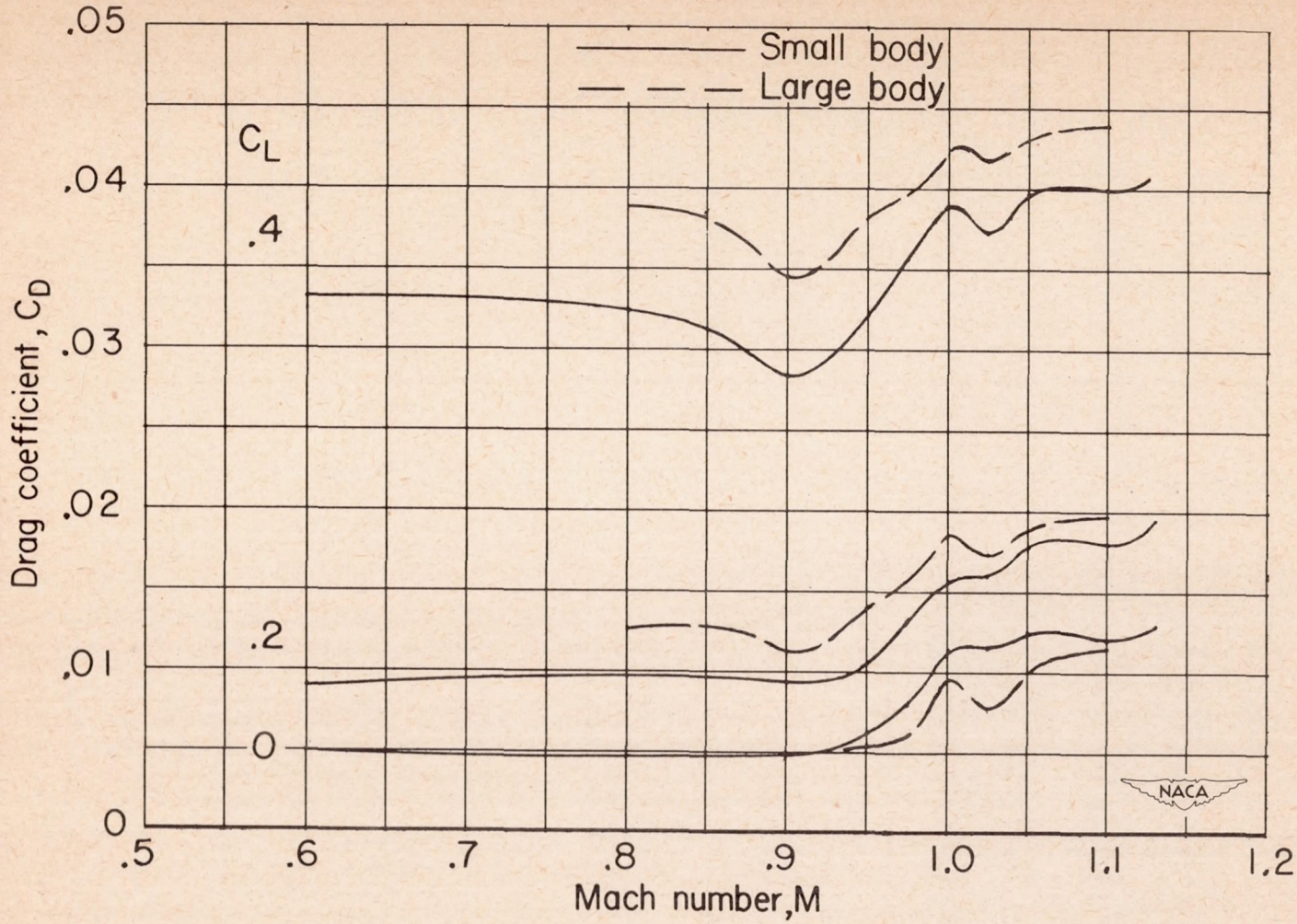

Figure 14.- Variation of drag coefficient with Mach number for the wing with interference when mounted on a small and a large body of similar shape.

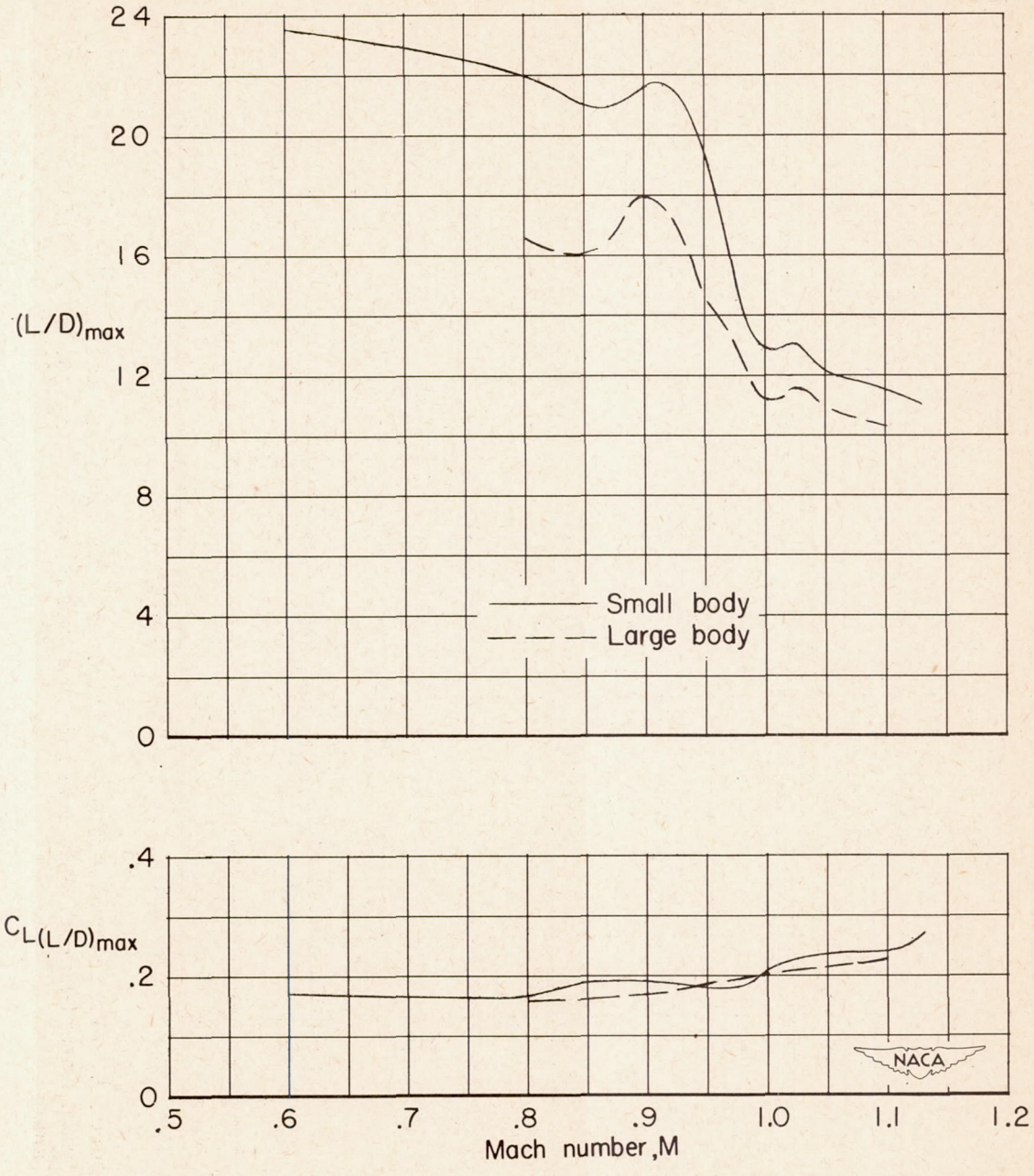

Figure 15.- Variation of maximum lift-drag ratio and lift coefficient for maximum lift-drag ratio with Mach number for the wing with interference when mounted on a small and a large body of similar shape.

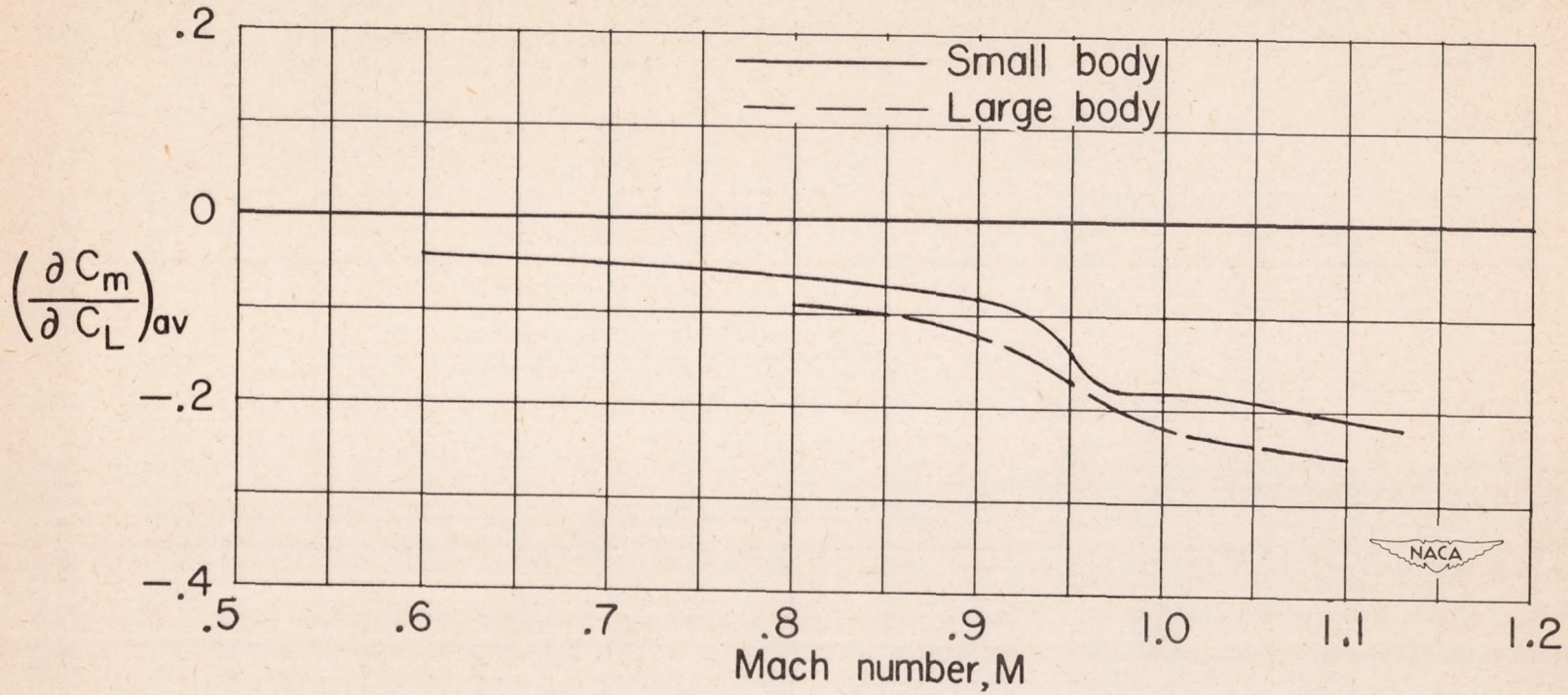

Figure 16.- Variation of average slope for the static longitudinal stability curve with Mach number for the wing with interference when mounted on a small and a large body of similar shape.